Available online at www.sciencedirect.com
ScienceDirect
Journal of Power Sources 172 (2007) 901–907
JOURNAL OF POWER SOURCES
www.elsevier.com/locate/jpowsour

Effects of functional electrolyte additives for Li-ion batteries

Eun-Gi Shim [a], Tae-Heum Nam [a], Jung-Gu Kim [a,*], Hyun-Soo Kim [b], Seong-In Moon [b]

[a] *Department of Advanced Materials Engineering, Sungkyunkwan University, Suwon 440-746, Republic of Korea*
[b] *Battery Research Group, Korea Electrotechnology Research Institute, Changwon 641-120, Republic of Korea*

Received 22 March 2007; received in revised form 18 April 2007; accepted 25 April 2007
Available online 13 May 2007

Abstract

The electrochemical behaviour and thermal stability of functional electrolyte additives for Li-ion batteries is investigated. The Li-ion cell systems is comprised of an anode of mesocarbon microbeads (MCMB) and a cathode ($LiCoO_2$) in a solution of 1.1 M $LiPF_6$ dissolved in ethylene carbonate and ethylmethyl carbonate (EC:EMC; 4:6, v/v). Vinyl acetate (VA) and vinylene carbonate (VC) in an ionic electrolyte containing triphenylphosphate (TPP) are tested as functional electrolyte additives. The main analysis tools used in this study are cyclic voltammetry (CV), differential scanning calorimetry (DSC), electrochemical impedance spectroscopy (EIS), and scanning electron microscopy (SEM). Cells containing VA or VC exhibit excellent irreversible capacity, coulombic efficiency, rate capability and cycleability. These features confirming the effectiveness of VC addition for improving both the cell performance and the thermal stability of electrolytes in TPP-containing solutions for Li-ion batteries.

Keywords: Lithium-ion batteries; Functional electrolyte additives; Vinyl acetate; Vinylene carbonate; Triphenylphosphate

1. Introduction

Lithium-ion batteries are the most suitable energy-storage systems for many portable electronic devices, such as cellular phones, digital cameras and notebooks because of their high specific energy and specific power [1]. Recently, non-flammable electrolytes with flame-retardants (FRs) have been reported to reduce electrolyte flammability, but FRs have negative effects on battery performance (especially cycle-life) due to their reactivity with the active materials in Li-ion cells [2–4]. To improve the performance of Li-ion batteries, functional electrolytes, such as vinylene carbonate (VC) [5,6], vinyl acetate (VA) [7,8], vinyl ethylene carbonate (VEC) [9], ethylene sulfite (ES) [10,11] and propylene sulfite (PS) [12], have been investigated. Yoshimoto et al. [5] reported that both charge and discharge performance were improved by the addition VC in a gel electrolyte that contained trimethyl phosphate (TMP). Abe et al. [8] found VA to be an effective additive because a VA-derived film has lower impedance and a more stable solid electrolyte interface (SEI) film, and also consists mainly of organic compounds with minimal content of inorganic species such as lithium and fluoride.

The present work involves a study of the influence of two functional electrolyte additives, namely, vinyl acetete (VA) and vinylene carbonate (VC), on the electrochemical performance of the Li-ion cells.

2. Experimental

Charge–discharge experiments were carried out using a two-electrode system, in a 2032 coin-type cell with a can diameter of 2.0 cm and a height of 0.32 cm. In the Li-ion cell, mesocarbon microbeads (MCMB) and $LiCoO_2$ were used as the anode and the cathode materials, respectively. In order to determine the effect of the additives, 1 wt.% VA or VC was added to blank electrolytes of 1.1 M $LiPF_6$/EC:EMC (4:6, v/v) +3 wt.% TPP (EC: ethylene carbonate; EMC:ethyl methyl carbonate; TPP: triphenylphosphate). A 1.1 M $LiPF_6$/EC:EMC (4:6, v/v) solution without any additive was used as a reference. Four different electrolyte compositions were selected, as listed in Table 1. Electrolyte 1 (E1) was the reference 1.1 M $LiPF_6$/EC:EMC (4:6, v/v) solution. Electrolyte 2 (E2) was formed by the addition of 3 wt.%

* Corresponding author. Tel.: +82 31 290 7360; fax: +82 31 290 7371.
E-mail address: kimjg@skku.ac.kr (J.-G. Kim).

0378-7753/$ – see front matter © 2007 Published by Elsevier B.V.
doi:10.1016/j.jpowsour.2007.04.089

Table 1
Electrolyte compositions

Electrolyte	Composition no.
E1	1.1 M $LiPF_6$/EC:EMC 4:6 (v/v)
E2	1.1 M $LiPF_6$/EC:EMC 4:6 (v/v) + TPP 3% (w/w)
E3	1.1 M $LiPF_6$/EC:EMC 4:6 (v/v) + TPP 3% (w/w) + VA 1% (w/w)
E4	1.1 M $LiPF_6$/EC:EMC 4:6 (v/v) + TPP 3% (w/w) + VC 1% (w/w)

TPP to electrolyte 1. Electrolyte 3 (E3) or electrolyte 4 (E4) were created by adding VA or VC to electrolyte 2 (E2), respectively. A porous polypropylene film was used as the separator. To insure reproducibility, at least three replicates were run for each cell. Cells were assembled in a dry room with a dew point below −55 °C.

To investigate the electrochemical stability of the additive-containing electrolytes, cyclic voltammetric (CV) measurements were conducted using a three-electrode cell. A glassy carbon electrode was used as the working electrode, with lithium as both the counter electrode and the reference electrode. The potential was scanned between 0 and 5.5 V versus Li/Li^+ at a sweep rate of 1 mV s^{-1}. The CV measurements were performed by means of a VMP2 multi-channel potentiostat (EG&G). The thermal stability of the electrolytes was measured using differential scanning calorimeter (DSC) at a heating rate of 5 °C min^{-1}, from 25 to 350 °C. The DSC measurements were conducted with DSC6200 equipment (SEICO Instruments Inc., Japan).

The rate capability of the cells was evaluated via a constant-current discharge at four current drains, namely: 0.6 mA (0.2*C*), 1.5 mA (0.5*C*), 3.0 mA (1*C*) and 6.0 mA (2*C*). All batteries were charged to 4.2 V with a constant-current/constant-voltage (CC/CV) protocol and then discharged to 2.75 V at different current rates. Cell cycle-life tests were performed with additive-free and additive-containing solutions. The cycling experiments were carried out by repeatedly charging and discharging at a current of 3.0 mA in the voltage range of 2.75–4.2 V. Before evaluating the electrochemical performance, the cells were activated through four charge–discharge cycles at the 0.1*C* rate. Cycling tests were performed with the VMP2 potentiostat system. All experiments were conducted under ambient conditions.

The cells were subject to electrochemical impedance spectroscopy (EIS) analysis using a VMP2 system. The frequency was varied from 100 to 0.01 Hz and the amplitude was set at 10 mV. The impedance data were analyzed using the ZSimpWin version 3.00 software. All potentials are reported with respect to the Li/Li^+ electrode potential. The electrode surface was observed with scanning electron microscopy (SEM) before and after cycling in different electrolytes.

3. Results and discussion

To measure the electrochemical stability of the additive-containing electrolytes, CV was conducted in the potential range of 0–5.5 V in the reference electrolyte without any additive (E1), the blank TPP-containing electrolyte (E2), and VA- and VC-containing electrolytes in blank electrolyte (E3 and E4, respectively), as shown in Fig. 1. No distinct oxidation peaks are observed up to 5.0 V versus Li/Li^+. This demonstrates the excellent electrochemical stability of the four electrolyte solutions. Note a key criterion for a Li-ion cell electrolyte is stability to oxidation up to 4.3 V versus Li/Li^+ [13].

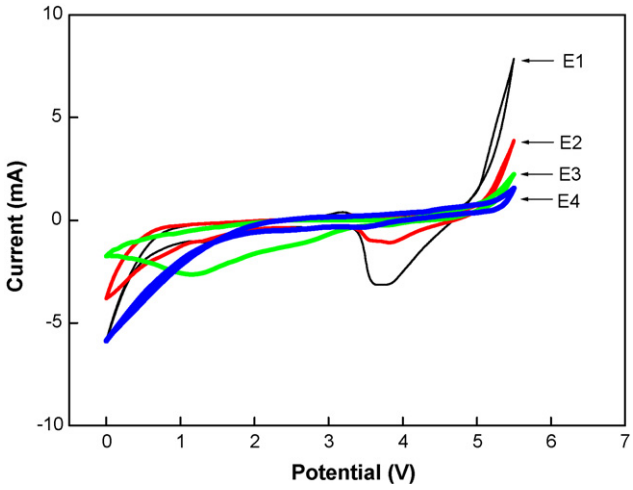

Fig. 1. Cyclic voltammograms of cells in four electrolytes: 1.1 M $LiPF_6$/EC:EMC (4:6) (reference, E1), reference +3% TPP (blank, E2), blank +1% VA (E3) and blank +1% VC (E4). Scan rate: 1 mV s^{-1}.

The DSC scans for the four electrolytes case presented in Fig. 2. Endothermic peaks are observed at about 196 and 216 °C in E1 and E2, respectively. In E3 and E4, the reaction temperature was 200 and 220 °C, respectively, confirming the higher thermal stability of the solutions containing a VA or VC additive compared with the E1 electrolyte. Furthermore, the VC-containing solution (E4) has the best thermal stability.

The initial charge–discharge profiles of the MCMB/$LiCoO_2$ cells in four different electrolytes are displayed in Fig. 3. The discharge capacities of E1, E2, E3 and E4 were 3.22, 2.75, 3.10 and 3.27 mAh, respectively, while the corresponding irreversible capacities were 0.39, 0.83, 0.72, and 0.31 mAh, to produce ini-

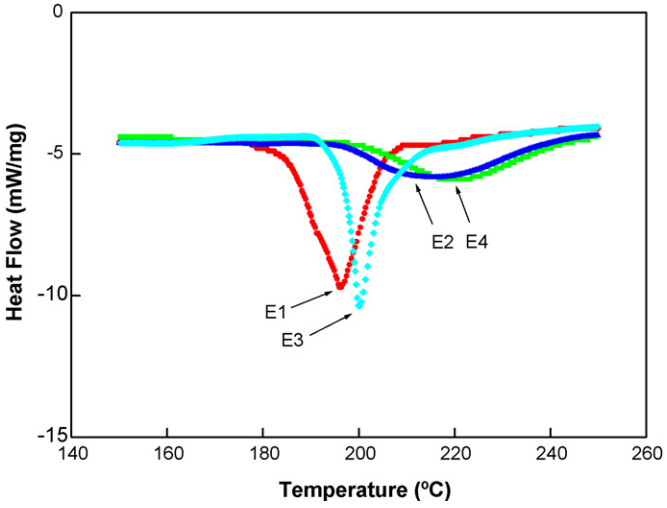

Fig. 2. Differential scanning calorimetry profiles of cells in four electrolytes: 1.1 M $LiPF_6$/EC:EMC (4:6) (reference, E1), reference +3% TPP (blank, E2), blank +1% VA (E3) and blank +1% VC (E4).

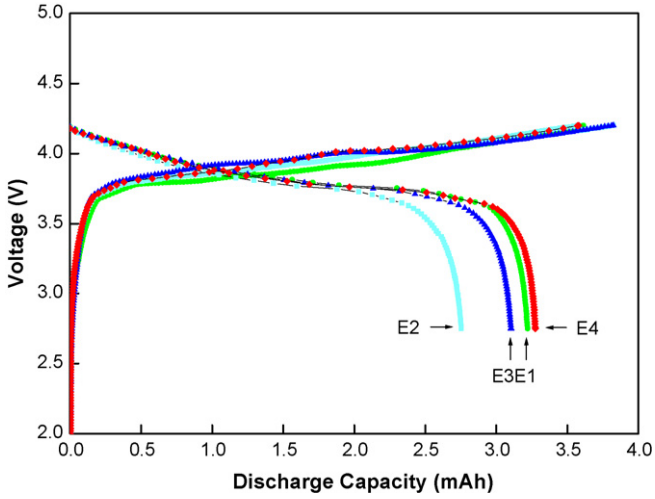

Fig. 3. Initial charge–discharge profiles of MCMB/$LiCoO_2$ cells in four electrolytes: 1.1 M $LiPF_6$/EC:EMC (4:6) (reference, E1), reference + 3% TPP (blank, E2), blank + 1% VA (E3) and blank + 1% VC (E4).

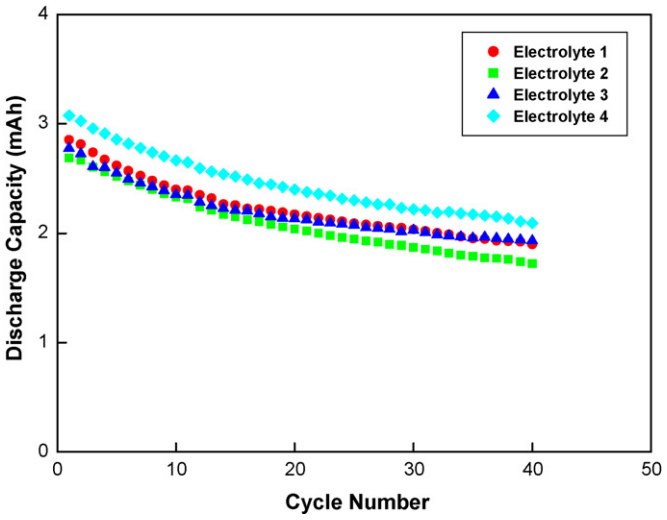

Fig. 5. Cycle performance of MCMB/$LiCoO_2$ cells at 1.0*C* rate.

tial coulombic efficiencies of 89, 77, 81 and 91%. These results demonstrate that the lowest discharge capacity of 2.75 mAh and coulombic efficiency of 77% is obtained with the blank TPP electrolyte (E2) without the VA or VC additive. Both the discharge capacity (3.10 or 3.27 mAh) and the coulombic efficiency (81 or 91%) are significantly improved by 1% VA or VC addition. The irreversible capacity may be associated with the structural change of $LiCoO_2$ and/or the SEI film formation reaction on the electrode surface [11]. By comparison, the cell performance of the experimental electrolytes in terms of reversible capacity and coulombic efficiency in the initial cycle deteriorated in the following order: E4 > E1 > E3 > E2. Hence, these studies indicate that VC addition decreases the surface impedance of the electrodes, and suppresses the irreversible capacity.

The effect of the different discharge rates, namely 0.2, 0.5, 1 and 2*C* is shown in Fig. 4. Both capacity and voltage decreases with increasing discharge current. This result can be explained in terms of electrode polarization due to an increased IR drop [14]. In this work, E1 exhibits the best rate capability (92.8% capacity retention at the 2*C* rate). E2 produced unsatisfactory results in terms of rate capability (87.0% capacity retention at the 2*C* rate). The rate capability of E3 with the VA additive (87.3% capacity retention at the 2*C* rate) is similar to that of E2, whereas that of E4 with the VC additive (92.2% capacity retention at 2*C* rate) is improved in comparison with E2. In

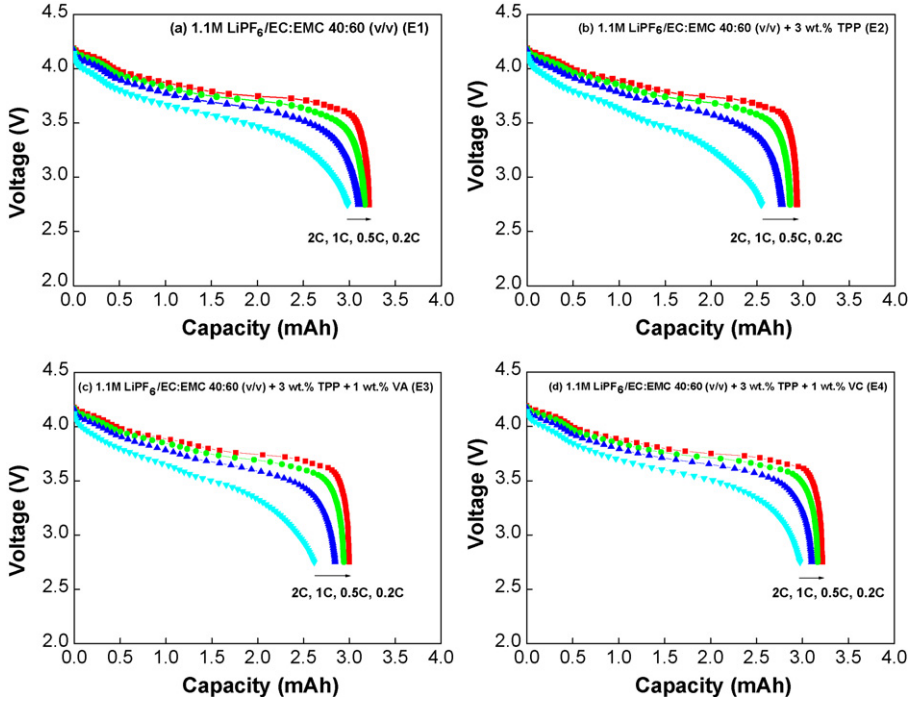

Fig. 4. Discharge capacity of MCMB/$LiCoO_2$ cells at various discharge rates after charging at 0.2*C* rate in four different electrolytes.

summary, the rate capability worsened in the following order: E1 > E4 > E3 > E2.

Electrochemical cycling tests were conducted with the four different electrolytes at the 1*C* rate, as shown in Fig. 5. The discharge capacities of the cells gradually degrade with increasing cycle number. The discharge capacity reaches a maximum for the cell with the VC-containing electrolyte (E4) after 40 cycles, and a minimum in the cell cycled in E2. These results suggest that the surface film formed on the electrode of the VC-containing electrolytes has the highest conductivity. The cycle capacity of the four electrolytes after 40 cycles decreases in the following order: E4 > E3 > E1 > E2. In addition, E1, E2, E3 and E4 exhibit a capacity fade of 33.5, 36.0, 30.5 and 31.9% of the initial capacity after 40 cycles, respectively, which confirms the improved cycling performance of E3 and E4 compared with E1 and E2. The cell with the VA-containing solution (E3) shows a slightly, but not significantly, better cycling performance than that of the VC-containing solution (E4). The cycleability of the four electrolytes deteriorates in the following order: E3 > E4 > E1 > E2. This capacity fading is accompanied by an increase in the internal impedance of the battery during cycling [15]. Balakrishnan et al. [16] postulated that the reduced cell performance is due to either electrochemical instability (which leads to capacity fading) or increased additive viscosity (which affects capacity utilization and power).

The above electrochemical cell measurements therefore indicate that the VA additive is effective in suppressing electrolyte decomposition on graphitic carbon and improving the cycleability because the additive decomposes earlier than solvents and forms a stable SEI film on the anode surface [8]. VC reacts predominantly on the surface of the electrodes, and its presence in the solutions has two positive effects; namely, decreasing the irreversible capacity of these electrodes and improving their cycleability (capacity, reversibility) [6].

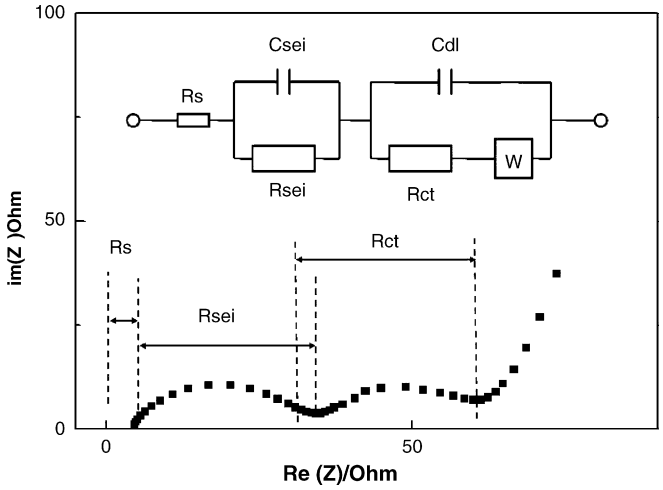

Fig. 6. Typical EIS result of Li-ion cell and an equivalent circuit used for EIS analysis.

In addition to the cycling test, impedance measurements were also performed on the Li-ion cells during 40 cycles. A typical EIS result of the Li-ion cells and an equivalent circuit used for the EIS analysis are shown in Fig. 6. The EIS of the Li-ion cells is composed of two partially overlapping semicircles and a straight sloping line at the low-frequency end [17]. In general, R_s is the electrolyte resistance of the cell. R_{sei} and C_{sei} are the resistance

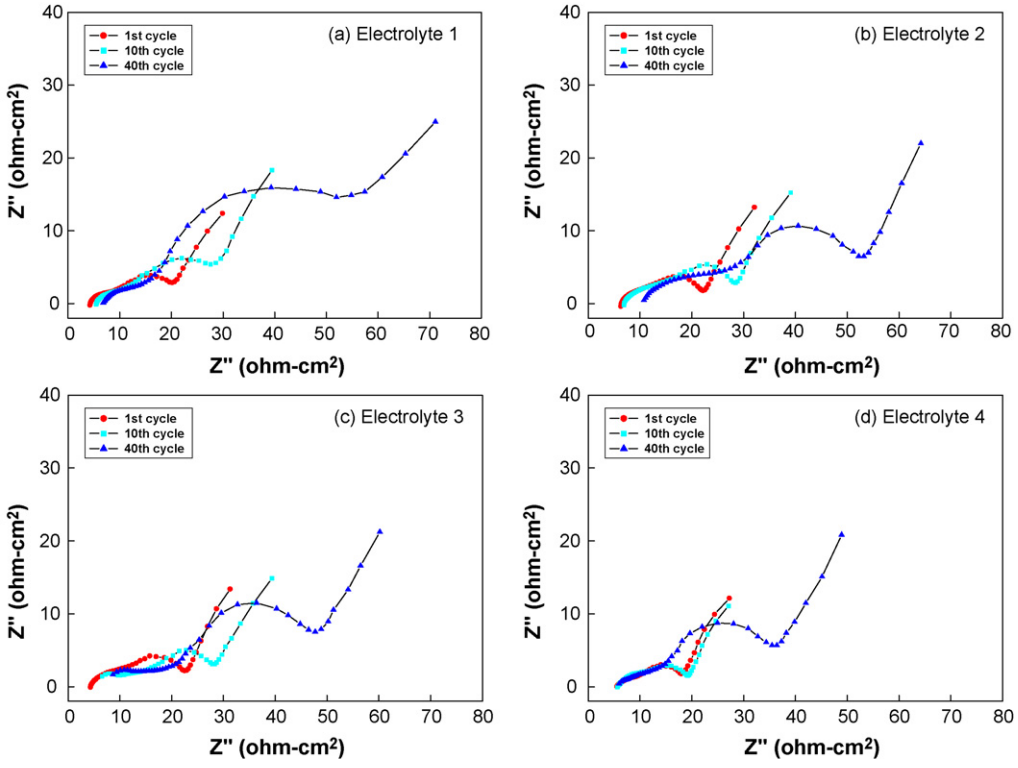

Fig. 7. Nyquist plots obtained from charged state of 4.2 V in four different electrolytes during cycling at 1.0*C* rate.

and capacitance of the SEI film, which correspond to the semicircle at high frequencies. R_{ct} and C_{dl} are the charge-transfer resistance and its relative double-layer capacitance, respectively, which correspond to the semicircle at medium frequencies. W is the Warburg impedance and is related to the effect of the diffusion of lithium ions on the interface between the active material particles and electrolyte, which corresponds to the straight sloping line at the low-frequency end. Since R_s and R_{sei} are of ohmic nature, their combination is called an ohmic impedance. The combination of R_{ct} and W is called Faradic impedance, which reflects the kinetics of the cell reactions [17,18].

The ac impedance spectra of the MCMB/$LiCoO_2$ cells on cycling in the additive-free and additive-containing solutions are shown in Fig. 7. The cell resistance ($R_{cell} = R_s + R_{sei} + R_{ct}$) values obtained in the charged state (4.2 V) of the cells on cycling are shown in Fig. 8. As indicated in Figs. 7 and 8, the cell resistance increases during the cycling process. The cell resistance R_{cell} of the four electrolytes after 40 cycles decreases in the following order: E2 > E1 > E3 > E4, as shown in Fig. 8. The data presented in Fig. 5 show that the cell with the VC-containing electrolyte (E4) gives the highest discharge capacity. The impedance of this E4 cell is the smallest during prolonged cycling. The EIS test results are therefore similar to those of the cycling tests.

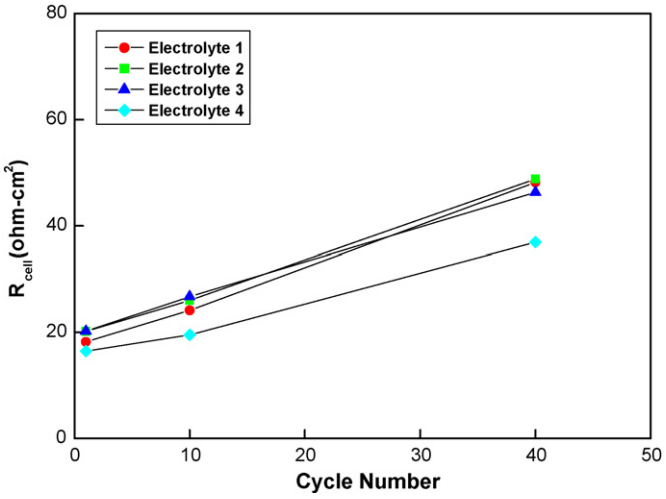

Fig. 8. Variation of R_{cell} values obtained from charged state of 4.2 V in four different electrolytes during cycling at 1.0*C* rate.

In order to investigate the effect of the additives on the morphology of the electrode before and after 40 cycles, the MCMB electrode was subjected to investigation by SEM, as shown in Fig. 9. The pristine electrode exhibites a smooth and clean surface, as shown in Fig. 9(a). The surfaces of the cycled elec-

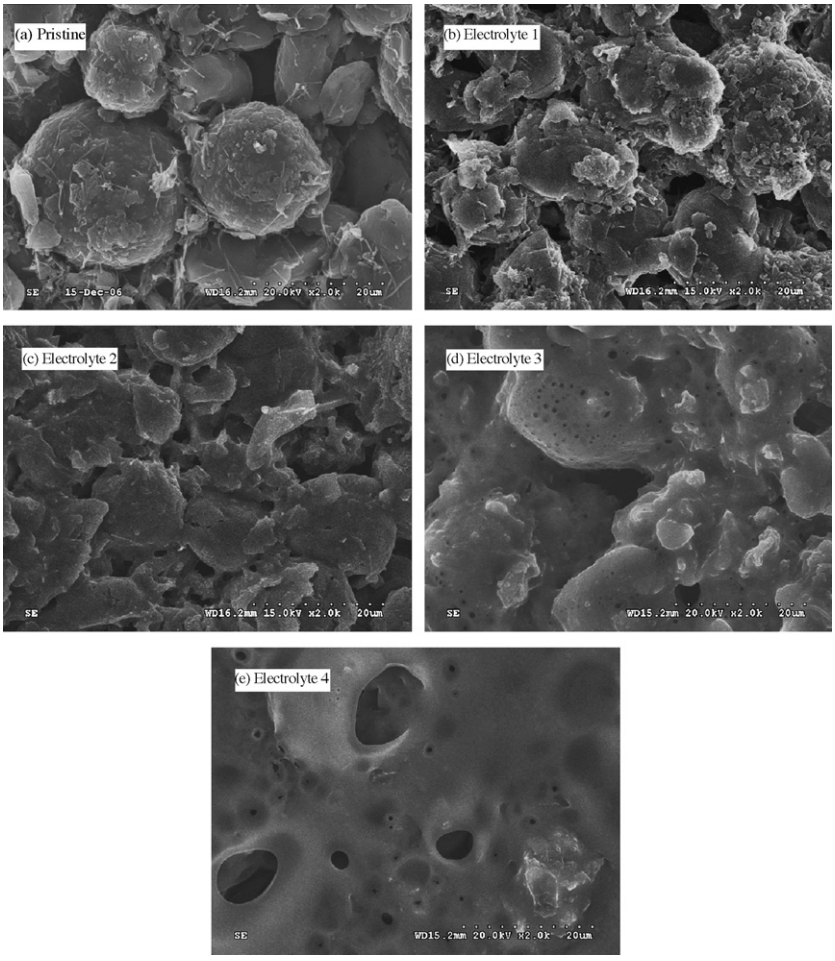

Fig. 9. Scanning electron micrographs of MCMB electrodes: (a) pristine electrode, and electrodes cycled in electrolytes (b) E1, (c) E2, (d) E3 and (e) E4.

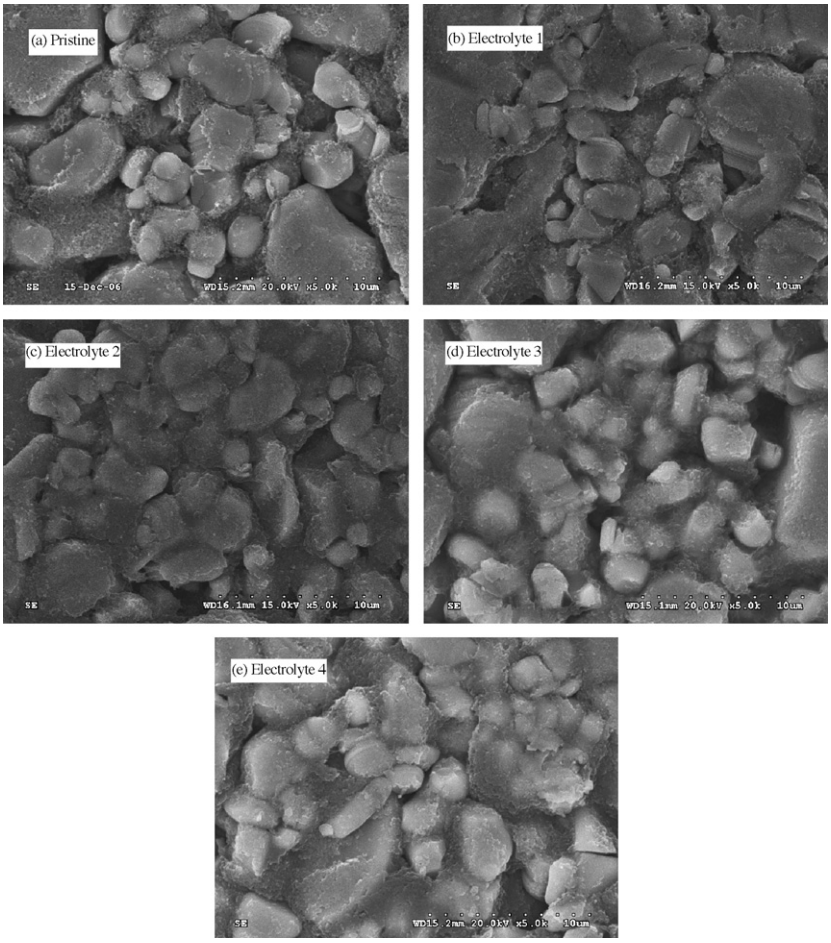

Fig. 10. Scanning electron micrographs of $LiCoO_2$ electrodes: (a) pristine electrode, and electrodes cycled in electrolytes (b) E1, (c) E2, (d) E3 and (e) E4.

trodes are covered with a uniformly distributed SEI layer after cycling. The micrographs of the cycled electrodes in VA- and VC-containing solutions (Fig. 9(d and e)) are, however, quite different from those of E1 and E2 (Fig. 9(b and c)). The thick VA-derived [7,8] and VC-derived [19] SEI films are evident in Fig. 9(d and e). In particular, the electrode cycled in the VC-containing solution (E4) has a surface that is fully covered by a polymer film, due to polymerization of the VC. It is assumed that the VC-derived surface film, consisting of a polymeric species, suppresses the deleterious reaction between the deposited lithium and electrolyte [19].

Scanning electron micrographs of the $LiCoO_2$ electrode before and after 40 cycles are presented in Fig. 10. Visible changes can be seen between the electrodes cycled in the four electrodes (Fig. 10(b–e)), the pristine electrode (Fig. 10(a)). Thick films covered most of the particles of the cycled electrodes. These SEM results indicate that prolonged cell cycling leads to the formation of a visible surface film on the cathode, which is significantly different to surface films on the anode.

4. Conclusions

The electrochemical and thermal properties of four functional electrolytes have been investigated. Solutions containing 1% VA or VC additive are electrochemically stable up to 5.0 V according to CV measurements. The thermal stability of the TPP-containing electrolyte is considerably improved by adding VA or VC to the solution. The VC-containing solution exhibits the best thermal stability.

The cell with VC-containing solution shows better electrochemical behaviour than that with the VA-containing solution, both on the initial charge–discharge and during the rate capability test. In cycling tests, the cells with VA- or VC-containing solutions give better cycling efficiency than a cell without additives. The cycleability does not differ significantly between the cells with VA- and VC-containing solutions. These results confirm the efficacy of VC as an additive for improving the cell performance and the thermal stability of electrolytes in TPP-containing solutions for Li-ion batteries.

Acknowledgments

Receipt of the electrolyte from TECHNO SEMICHEM Co., Ltd. is gratefully acknowledged.

References

[1] S.S. Zhang, K. Xu, T.R. Jow, J. Power Sources 160 (2006) 1349.
[2] K. Xu, M.S. Ding, S. Zhang, J.L. Allen, T.R. Jow, J. Electrochem. Soc. 149 (2002) A622.

[3] X.L. Yao, S. Xie, C.H. Chen, Q.S. Wang, J.H. Sun, Y.L. Li, S.X. Lu, J. Power Sources 144 (2005) 170.
[4] L. Xiao, X. Ai, Y. Cao, H. Yang, Electrochim. Acta 49 (2004) 4189.
[5] N. Yoshimoto, Y. Niida, M. Egashira, M. Morita, J. Power Sources 163 (2006) 238.
[6] D. Aurbach, K. Gamolsky, B. Markovsky, Y. Gofer, M. Schmidt, U. Heider, Electrochim. Acta 47 (2002) 1423.
[7] H.J. Santner, K.C. Möller, J. Ivančo, M.G. Ramsey, F.P. Netzer, S. Yamaguchi, J.O. Besenhard, M. Winter, J. Power Sources 119–121 (2003) 368.
[8] K. Abe, H. Yoshitake, T. Kitakura, T. Hattori, H. Wang, M. Yoshio, Electrochim. Acta 49 (2004) 4613.
[9] Y. Hu, W. Kong, H. Li, X. Huang, L. Chen, Electrochem. Commun. 6 (2004) 126.
[10] G.H. Wrodnigg, J.O. Besenhard, M. Winter, J. Power Sources 97-98 (2001) 592.
[11] M. Itagaki, N. Kobari, S. Yotsuda, K. Watanabe, S. Kinoshita, M. Ue, J. Power Sources 148 (2005) 78.
[12] G.H. Wrodnigg, T.M. Wrodnigg, J.O. Besenhard, M. Winter, Electrochem. Commun. 1 (1999) 148.
[13] R.M. Millan, H. Slegr, Z.X. Shu, W. Wang, J. Power Sources 81–82 (1999) 20.
[14] S.S. Zhang, K. Xu, T.R. Jow, J. Power Sources 140 (2005) 361.
[15] D. Zhang, B.S. Haran, A. Durairajan, R.E. White, Y. Podrazhansky, B.N. Popov, J. Power Sources 91 (2000) 122.
[16] P.G. Balakrishnan, R. Ramesh, T.P. Kumar, J. Power Sources 155 (2006) 401.
[17] S.S. Zhang, K. Xu, T.R. Jow, Electrochim. Acta 49 (2004) 1057.
[18] S. Yang, H. Song, X. Chen, Electrochem. Commun. 8 (2006) 137.
[19] H. Ota, K. Shima, M. Ue, J.I. Yamaki, Electrochim. Acta 49 (2004) 565.